

Post-print of "SM Mirfalah-Nasiri, A Basti, [R Hashemi](#) (2016) Forming limit curves analysis of aluminum alloy considering the through-thickness normal stress, anisotropic yield functions and strain rate, International Journal of Mechanical Sciences, Volume 117, Pages 93-101.

<https://doi.org/10.1016/j.ijmecsci.2016.08.011>

## Forming limit curves analysis of AA3104-H19 considering the through-thickness normal stress and anisotropic yield functions

S.M. Mirfalah Nasiri<sup>1</sup>, A. Basti<sup>\*1</sup>, R. Hashemi<sup>2</sup>

*1- Department of Mechanical Engineering, University of Guilan, Rasht, Iran*

*2- School of Mechanical Engineering, Iran University of Science and Technology, Tehran, Iran*

### **Abstract**

Based on three anisotropic yield criteria including Karafillis-Boyce (K-B), Yld96 and Yld2011, directional normalized uniaxial yield stresses, directional r-value and forming limit curve (FLC) for AA3104-H19 aluminum alloy under plane stress condition are numerically investigated in this article. Moreover, considering through-thickness normal stress effect the forming limit diagram (FLD), stress-based forming limit diagram (FLSD) and extended forming limit stress diagram (XFLSD) is also studied theoretically based on Yld2011 yield criterion and modified Marciniak–Kuczynski (M–K) model. The nonlinear equations set are solved employing Newton–Raphson numerical method to calculate limiting strains. The anisotropic plastic behavior and FLC of AA3104-H19 predicted by Yld2011 yield criterion is in good agreement with experimental data and is more accurate than those of K-B and Yld96 yield functions. In addition, according to FLD, the formability of sheet metal increases by applying the through-thickness normal stress. The effects of strain rate at quasi-static condition and temperature are theoretically investigated on the FLD of AA3104 sheets. The positive temperature sensitivity and negative strain rate sensitivity are observed of FLD of AA3104 alloy.

**Keywords:** Forming Limit Curve, Through-Thickness Normal Stress, Yld2011 Yield Function, Anisotropic Aluminum Alloy, Strain Rate Sensitivity.

---

\*Corresponding author. Tel./fax: +98 13 33690276.  
E-mail address: [basti@guilan.ac.ir](mailto:basti@guilan.ac.ir) (A.Basti).

Nomenclature	
$\psi$	Yield function
$Y$	Yield stress
$\mathbf{S}$	Isotropic plasticity equivalent (IPE) stress tensor
$\boldsymbol{\sigma}$	Cauchy stress tensor
$\mathbf{L}$	Linear-transformation tensor
$a$	Material coefficient of Yld96, K_B and Yld2011 criterions
$\alpha_k, k = 1,2,3$	Weight factors of Yld96 criterion
$\alpha_i, i = x, y, z$	Anisotropic coefficients of Yld96 criterion
$\beta_i, i = 1,2,3$	Angle between the principal directions of $\mathbf{S}$ and the anisotropic axes
$\mathbf{p}$	Transformation matrix
$S_i, i = 1,2,3$	Principal values of the IPE stress tensor
$c_i, i = 1,2, \dots, 6$	Material parameters of Yld96 criterions
$c$	Weight factors of K_B criterion
$\mathbf{S}', \mathbf{S}'' \text{ and } \mathbf{S}'''$	Linear transformation IPE stress tensor
$S'_i, S''_i \text{ and } S'''_i, i = 1,2,3$	Principal values of $\mathbf{S}', \mathbf{S}'' \text{ and } \mathbf{S}'''$
$C'_{ij}, i = j = 1,2, \dots, 6$	Material parameters of Yld2011 criterions
$\xi$	Scalar quantity of Yld2011 criterions
$t_0$	Initial thickness
$f_0$	Initial imperfection factor
$f$	Imperfection factor
$\theta$	Groove angle
$\varepsilon_i, i = 1,2,3$	Principal strain components in the material coordinates ( $xyz$ )
$d\varepsilon_i, i = 1,2,3$	Strain increments in the material coordinates ( $xyz$ )
$d\varepsilon_{nn}, d\varepsilon_{tt}, d\varepsilon_{nt}$	Strain increments in the groove coordinates ( $ntz$ )
$\bar{\varepsilon}$	Effective plastic strain
$d\bar{\varepsilon}$	Effective plastic strain increment
$\bar{\sigma}_Y$	Effective stress obtained from hardening law
$\bar{\sigma}$	Effective stress obtained from yield criterion
$\sigma_e$	Equivalent stress
$\sigma_{hyd}, \sigma_m$	Hydrostatic stress
$\sigma_i, i = 1,2,3$	Principal stress components in the material coordinates ( $xyz$ )

$\sigma_{nn}, \sigma_{tt}, \sigma_{nt}$	Stress components in the groove coordinates ( $ntz$ )
$\sigma_0, \sigma_{45}, \sigma_{90}$	Yield stresses in $0^\circ, 45^\circ$ and $90^\circ$ to the rolling direction
$r_0, r_{45}, r_{90}$	Anisotropic coefficients ( $r$ -values) in $0^\circ, 45^\circ$ and $90^\circ$ to the rolling direction
$\gamma, S$	Non-dimensional parameters in the M_K model at normal stress
$R$	Rotation matrix in the M_K model
$J$	Jacobin matrix
$A$	Initial yield strength of the material at room temperature
$B, K$	Work hardening coefficient
$C, m_L$	Strain-rate sensitivity coefficients
$n, n_L$	Strain hardening coefficients
$m$	Material constant in Johnson-Cook equation
$\dot{\epsilon}$	Equivalent plastic strain rate
$\dot{\epsilon}_0$	Reference strain rate
$T_m$	Melting temperature of the material
$T_r$	Room temperature
$T$	Current temperature

## 1-Introduction

The forming limit curve is established experimentally and numerically in terms of principle strains to predict the strain level, the onset of plastic instability (necking) or fracture and the range of safety. The expensive experimental tests can be saved by introducing the theoretical predictive FLC model and a wide range of forming conditions can be simulated. For these reasons, the FLC is very useful in the formation of metal sheets. Many researches employed the Marciniak–Kuczynski model to predict the onset of plastic instability (necking) in sheet metal forming. Keeler and Backofen [1] discovered and initially developed the forming limit diagram to predict the onset of plastic instability and were extended by Goodwin [2], Marciniak and Kuczynski [3, 4].

Because of strongly anisotropic behavior of sheet metals in cold rolling process, the proper yield functions have significant effect on the accuracy of FLC. The effects of different yield functions on the FLCs for sheet metals were investigated. The effects of two non-quadratic yield criteria, Yld96 and BBC2000, and Voce hardening law in conjunction with the M-K theory for orthotropic sheet metals under plane stress condition were investigated by Butuc et al. [5] to predict the FLCs. In addition, yield surface shape, yield stress and  $r$ -value directionalities of Yld96 and BBC2000 were experimentally conducted. Prediction of FLD by considering the Hosford and BBC2000 yield criteria based on M-K model was studied by Ganjani and Assempour [6]. They concluded that for AK steel, Hosford yield

Post-print of "SM Mirfalah-Nasiri, A Basti, [R Hashemi](#) (2016) Forming limit curves analysis of aluminum alloy considering the through-thickness normal stress, anisotropic yield functions and strain rate, International Journal of Mechanical Sciences, Volume 117, Pages 93-101.

<https://doi.org/10.1016/j.ijmecsci.2016.08.011>

criterion with the exponent 6 predicts the FLDs and for AA5XXX alloy, both BBC2000 yield function and Hosford yield function with the exponent 8 predict limit strains which have good agreement with the experimental data. Ahmadi et al. [7] investigated the effects of BBC2000, BBC2002 and BBC2003 and Voce and Swift hardening law based on M-K method for AA3003-O aluminum alloy. They showed that the theoretical obtained results have satisfactory agreement with the experimental ones. The performance and capability of five yield criteria including Hill's 48, Hill's 90, Hill's 93, Yld89 and Plunkett to predict the forming limit diagram of the AA5754 aluminum sheet metal was carried out by Dasappa and et al. [8]. They found that the prediction of FLD highly depends on the yield surface shape and the method of determining the material parameters. The experimental and theoretical investigation of forming limit diagram of AA-Li2198 aluminum alloy by considering von Mises, Hill'48, Hosford and Barlat 89 yield functions based on M-K model was studied by Li et al. [9]. The results show that, based on Hosford yield criterion the left hand side of FLC including the tension-compression strain states has better agreement with experimental results and based on Hill'48 yield criterion the right hand side of FLC including tension-tension strain states has more satisfactory accurate with experimental data. The experimental and numerical studies of FLD and FLSD by applying of von Mises, Hill's 48 and Yld2000 with Voce and Swift hardening law based on M-K approach were carried out by Panich et al. [10]. Comparison of theoretical results and experimental data shows that the stress based forming limit diagram has strongly affected the yield criterion and hardening model. Ozturk et al. [11] investigated the capability of different yield criteria including Hill-48, Barlat 89, and YLD2000 based on M-K theory in order to predict the forming limit diagram for high strength steel sheet. They observed that the prediction of FLD by considering the Yld2000 has better agreement with experimental data.

Using strain based forming limit diagram by assuming the in plane stress is responsible for the widespread prediction of forming limit sheet metals. However, in some industrial forming of metal such as hydroforming, the normal stress effect should be considered due to high level of the fluid pressure. Bridgman [12] examined the material response of very high hydrostatic pressure and indicated that the ductility of material increases under hydrostatic pressure. Fuchs [13] introduced double-sided hydraulic pressure to a tubular hydroforming operation and observed that the ratio of stress,  $\gamma$ , has remarkable efficient on the expansion of tube. Considering the effect of normal stress, the formability of sheet metals was investigated based on Hill modeling and Swift modeling and Marciniak-Kuczynski approach.

The influence of normal stress on FLD based on M-K model for AA6011 and STKM-11A were considered and compared to experimental data by Assempour et al. [14]. They observed that by increasing the normal compressive stress the FLD shifts up and the formability of sheet metals would increase. Hashemi and Abrinia [15] considered the effect of strain path by applying two type of pre-

Post-print of "SM Mirfalah-Nasiri, A Basti, [R Hashemi](#) (2016) Forming limit curves analysis of aluminum alloy considering the through-thickness normal stress, anisotropic yield functions and strain rate, International Journal of Mechanical Sciences, Volume 117, Pages 93-101.

<https://doi.org/10.1016/j.ijmecsci.2016.08.011>

straining and through-thickness normal stress to predict the FLC based on the modified M-K model. The effects of strain path non-linearity and the normal stress based on M-K theory were numerically carried out by Nurcheshmeh and Green [16] to predict the FLC for AISI-1012, AA6011 and STKM-11A, which showed a good accuracy and agreement in comparison between the numerical results and the experimental data. The effects of the through-thickness normal stress and material anisotropy on forming limit diagram based on M-K method with Barlat's anisotropic yield surface were studied numerically by Zhang et al. [17]. They showed that by increasing the through-thickness normal stress of AA5XXX and AA6011 aluminum alloy the limit strain and the formability of sheet metal would increase. Zhang et al. [18] were also investigated the influences of plane stress yield functions including Hill's 48, Barlat's 89 and Yld2003 yield criterion with M-K model on forming limit curve for AA6111-T3 aluminum alloy. Then the effect of through-thickness normal stress on traditional FLC, eFLC, FLSC and XSFLC was numerically carried out. The results showed that the Yld2003 provides better prediction than the Hill's 48 and Barlat's 89. Yang et al. [19] computed the FLDs of 5A06-O sheet at different temperatures by considering a modified M-K model combined with ductile fracture criterion. Employing a new computing method based on wide sheet bending test, the effect of different temperature was investigated to determine of the material constant of ductile fracture criterion and initial thickness imperfection parameter. Moreover, the influence of through-thickness normal stress on FLD was carried out experimentally and was compared to the results of simulation in Abaqus/Explicit.

Several experimentally researches have been carried out to understand the strain rate sensitivity on FLD for the strain rate sensitive materials using M-K model. Based on uniaxial tensile test, the effect of the strain rate on the formability of CQ and DP590 were experimentally performed by Kim et al. [20]. The results show that the strain rate has a significant effect on the formability of CQ and DP590 sheet metals. Employing Johnson-Cook constitutive law, Gerdooei and Dariani [21] were analytically investigated the effect of strain rate on FLD and were theoretically studied on dynamic instability of non-homogeneous OFHC copper metal sheets under biaxial stretching. Dariani et al. [22] were experimentally carried out the forming velocity sensitivity on FLD for Al6061-T6 and AISI1045 sheets. Johnson-Cook constitutive model and the Jones-Wilkins-Lee (JWL) model were used for metal sheets and the explosive charge respectively. They concluded that the impact loading has positive sensitivity on formability of both Al6061-T6 and AISI1045 sheets. The effects of strain rate ( $10^{-4}$  to  $10^0 \text{ s}^{-1}$ ) and temperatures (293–473 K) on FLD by using M-K method and Khan-Huang-Liang (KHL) constitutive model with YLD96 anisotropic yield surface were theoretically performed by Khan and Baig [23]. They observed the positive strain-rate sensitivity at 293 K and negative strain-rate sensitivity at 473 K on FLD for AA5182-O sheets. A modified Ludwick hardening law and M-K theory were employed to investigate the strain rate and

Post-print of “SM Mirfalah-Nasiri, A Basti, [R Hashemi](#) (2016) Forming limit curves analysis of aluminum alloy considering the through-thickness normal stress, anisotropic yield functions and strain rate, International Journal of Mechanical Sciences, Volume 117, Pages 93-101.

<https://doi.org/10.1016/j.ijmecsci.2016.08.011>

temperature effects of formability of sheet metal AA5086 by Chu et al. [24]. The experimental results show the positive sensitivity of temperature and negative strain rate on formability of sheet metal AA5086. Zhang et al. [25] were experimentally investigated the effects of strain rate (2.5, 120 and 150 s<sup>-1</sup>) and temperature (100, 200 and 300°C) of FLCs of AA5086 sheets using modified Voce constitutive model.

Because lack of proper implementation of classic yield criterion such as Von-Mises and Hill's 48 to predict the anisotropy plastic behavior and FLCs for anisotropic aluminum alloy sheet metals particularly, the advanced yield criterion was introduced to obtain satisfactory accuracy and agreement between the theoretical and experimental results. Moreover, in many of industrial application such as hydroforming the in plane stress theory is not a proper assumption and the normal stress effect should be implemented. According to what has been said, the yield surface prediction, directional normalized uniaxial yield stresses and directional r-value for AA3104-H19 are numerically investigated based on three anisotropic yield criterions including Karafillis-Boyce, Yld96 and Yld2011. Moreover, determination of the FLD based on the Marciniak and Kuczynski model and three anisotropic yield criterions under in plane stress conditions for AA3104-H19 aluminum alloy is also numerically carried out. Nevertheless, the effect of the through-thickness normal stress on the forming limit curve including forming limit diagram (FLD), stress-based forming limit diagram (FLSD) and extended stress-based forming limit diagram (XFLSD) is investigated based on modified M-K model and Yld2011 anisotropic yield criterions. Comparison between numerical results and available published experimental data shows that Yld2011 gives a better prediction than the Yld96 and K-B. Because of effective stress depended to strain rate, many researches consider this parameter in constitutive model and results show good agreement with experimental results. So, temperature and strain rate influence on AA3104 FLD are theoretically investigated. Results show that the formability of sheet metal increases with temperature and decreases with strain rate.

## **2- Anisotropic yield criterions**

The stress state corresponding to the onset of plastic deformation of material can be considered as yield surface. The yield function can be defined mathematically in terms of all stress components in the general implicit form.

$$\psi(\bar{\sigma}, Y) = \bar{\sigma} - Y = 0 \quad (1)$$

where quantity  $\bar{\sigma} \geq 0$  is the equivalent stress or effective stress and  $Y > 0$  is an arbitrary reference yield stress which is determined from a uniaxial tensile or compression test.

### **2-1- Barlat's 96 yield criterion**

Post-print of "SM Mirfalah-Nasiri, A Basti, [R Hashemi](#) (2016) Forming limit curves analysis of aluminum alloy considering the through-thickness normal stress, anisotropic yield functions and strain rate, International Journal of Mechanical Sciences, Volume 117, Pages 93-101.

<https://doi.org/10.1016/j.ijmecsci.2016.08.011>

According to the experimental investigations, the plastic behavior modeling of aluminum alloys is very difficult with Barlat's 1989 and Barlat's 1991 yield criterion. In order to overcome the applicability limits of these yield criterion, Barlat proposed a yield criterion so-called Yld96 using the weight factors [26].

$$\phi = \alpha_1 |S_1 - S_2|^a + \alpha_2 |S_2 - S_3|^a + \alpha_3 |S_3 - S_1|^a = 2\bar{\sigma}^a \quad (2)$$

where  $\alpha_1, \alpha_2$  and  $\alpha_3$  are the weight factors which are related to the anisotropy of the materials.  $a$  is a coefficient equals with 8 for FCC and 6 for BBC material.  $S_1, S_2$  and  $S_3$  are the principle are the principle value of the isotropic plasticity equivalent stress  $\mathbf{S}$  which is defined by the following linear transformation operator.

$$\mathbf{S} = \mathbf{L} : \boldsymbol{\sigma} \quad (3)$$

where  $\boldsymbol{\sigma}$  is the Cauchy stresses and  $\mathbf{L}$  is a fourth order tensor which is calculated as following

$$\mathbf{L} = \begin{bmatrix} \frac{c_2 + c_3}{3} & -\frac{c_3}{3} & -\frac{c_2}{3} & 0 & 0 & 0 \\ -\frac{c_3}{3} & \frac{c_3 + c_1}{3} & -\frac{c_1}{3} & 0 & 0 & 0 \\ -\frac{c_2}{3} & -\frac{c_1}{3} & \frac{c_2 + c_1}{3} & 0 & 0 & 0 \\ 0 & 0 & 0 & c_4 & 0 & 0 \\ 0 & 0 & 0 & 0 & c_5 & 0 \\ 0 & 0 & 0 & 0 & 0 & c_6 \end{bmatrix} \quad (4)$$

where  $c_i$  are the material parameters.  $\alpha_1, \alpha_2$  and  $\alpha_3$  define as following

$$\alpha_k = \alpha_x p_{1k}^2 + \alpha_y p_{2k}^2 + \alpha_z p_{3k}^2 \quad (5)$$

In Eq. (5)  $\mathbf{p}$  is the transformation matrix between the principle directions of stress tensor  $\mathbf{S}$  and principle axes of anisotropy.  $\alpha_x, \alpha_y$  and  $\alpha_z$  are the anisotropic variable quantities.  $\beta_i$  are the angle between the principal directions of  $\mathbf{S}$  and the anisotropic axes which are defined as

$$\begin{aligned} \alpha_x &= \alpha_{x0} \cos^2 2\beta_1 + \alpha_{x1} \cos^2 2\beta_1 \\ \alpha_y &= \alpha_{y0} \cos^2 2\beta_2 + \alpha_{y1} \cos^2 2\beta_2 \end{aligned} \quad (6)$$

$$\begin{aligned} \alpha_x &= \alpha_{z0} \cos^2 2\beta_3 + \alpha_{z1} \cos^2 2\beta_3 \\ \left\{ \begin{array}{l} \beta_i = 0 \rightarrow \alpha_{i0} = \alpha_i \\ \beta_i = \frac{\pi}{2} \rightarrow \alpha_{i1} = \alpha_i \end{array} \right. \end{aligned} \quad (7)$$

$$\begin{aligned} \cos^2 2\beta_1 &= \begin{cases} y.1, |S_1| \geq |S_3| \\ y.3, |S_1| < |S_3| \end{cases} \\ \cos^2 2\beta_2 &= \begin{cases} z.1, |S_1| \geq |S_3| \\ z.3, |S_1| < |S_3| \end{cases} \\ \cos^2 2\beta_3 &= \begin{cases} x.1, |S_1| \geq |S_3| \\ x.3, |S_1| < |S_3| \end{cases} \end{aligned} \quad (8)$$

Post-print of "SM Mirfalah-Nasiri, A Basti, [R Hashemi](#) (2016) Forming limit curves analysis of aluminum alloy considering the through-thickness normal stress, anisotropic yield functions and strain rate, International Journal of Mechanical Sciences, Volume 117, Pages 93-101.

<https://doi.org/10.1016/j.ijmecsci.2016.08.011>

The anisotropic material coefficients corresponding to the Yld96 yield criterion for AA3104-H19 aluminum alloy are presented in Table. 1.

### 2-2- Karafillis-Boyce (K-B) yield criterion

Karafillis-Boyce yield criterion is a linear transformation of isotropic to anisotropic case and a weighted combination of Tresca and Von-Mises yield criterions. The K-B yield function is defined as following form [26].

$$\frac{(1-c)\psi_1 + c\psi_2}{2} = \bar{\sigma}^a, \quad a > 2$$

$$\psi_1 = |S_1 - S_2|^a + |S_2 - S_3|^a + |S_3 - S_1|^a$$

$$\psi_2 = \frac{3^a}{2^{a-1} + 1} (|S_1|^a + |S_2|^a + |S_3|^a)$$
(9)

In Eq. (9)  $a$ ,  $c$  and  $S_i$  are the material coefficient, weighted coefficient and the principal values of the stress deviator respectively. The anisotropic material coefficients corresponding to the K-B yield criterion for AA3104-H19 aluminum alloy are presented in Table. 2.

### 2-3- Yld2011 yield criterion

The anisotropic Yld2011-18p yield criterion with 18 calibrated parameters to experimental data is a development of Yld2004-18p and anisotropic Yld2011-27p yield criterion with 27 calibrated parameters to experimental data is an expansion of Yld2011-18p [28]. The advantage of these yield criterions is the simple application in the commercial FEM software. The Yld2011-18p yield criterion with two linear transformations is defined according to

$$\bar{\sigma} = \left\{ \frac{1}{\xi} \left[ \sum_{i=1}^3 \sum_{j=1}^3 |S'_i + S''_j|^a \right] \right\}^{1/a} = \left\{ \frac{1}{\xi} \left[ |S'_1 + S''_1|^a + |S'_1 + S''_2|^a + |S'_1 + S''_3|^a + \right. \right.$$

$$\left. |S'_2 + S''_1|^a + |S'_2 + S''_2|^a + |S'_2 + S''_3|^a + |S'_3 + S''_1|^a + |S'_3 + S''_2|^a + |S'_3 + S''_3|^a \right] \right\}^{1/a}$$
(10)

where  $S'_i$  and  $S''_j$  are the linear transformation of the stress deviator, and  $a$  is the yield function exponent.

In Eq. (10), the scalar quantity  $\xi$  is computed as

$$\xi = \left(\frac{4}{3}\right)^a + 4\left(\frac{2}{3}\right)^a + 4\left(\frac{1}{3}\right)^a, \quad a \geq 1$$
(11)

Adding the third linear transformation to Yld2011-18p, the Yld2011-27p yield criterion can be presented as

$$\bar{\sigma} = \left\{ \frac{1}{\xi} \left[ \sum_{i=1}^3 \sum_{j=1}^3 |S'_i + S''_j|^a + \sum_{j=1}^3 |S'''_j|^a \right] \right\}^{1/a}$$
(12)

In Eq. (12) the scalar quantity  $\xi$  can be derived as

$$\xi = \left(\frac{4}{3}\right)^a + 5\left(\frac{2}{3}\right)^a + 6\left(\frac{1}{3}\right)^a, a \geq 1 \quad (13)$$

The linear transformation in Eq. (10) and Eq. (12) are defined in the following form.

$$\mathbf{S}' = \mathbf{C}':\mathbf{S}, \begin{bmatrix} S'_{11} \\ S'_{22} \\ S'_{33} \\ S'_{32} \\ S'_{31} \\ S'_{12} \end{bmatrix} = \begin{bmatrix} 0 & -C'_{12} & -C'_{13} & 0 & 0 & 0 \\ -C'_{21} & 0 & -C'_{23} & 0 & 0 & 0 \\ -C'_{31} & -C'_{32} & 0 & 0 & 0 & 0 \\ 0 & 0 & 0 & C'_{44} & 0 & 0 \\ 0 & 0 & 0 & 0 & C'_{55} & 0 \\ 0 & 0 & 0 & 0 & 0 & C'_{66} \end{bmatrix} \begin{bmatrix} S_{11} \\ S_{22} \\ S_{33} \\ S_{32} \\ S_{31} \\ S_{21} \end{bmatrix} \quad (14)$$

The material parameters in Eq. (14),  $C_{ij}$ , based on Yld2011-18p which is used in this article for AA3104-H19 aluminum alloy are presented in Table. 3.

### 3-M-K theory with normal stress

In this section, the Marciniak–Kuczynski model is extended considering the through-thickness normal stress. The M–K method is considered based on initial geometrical inhomogeneity or initial imperfection ( $f_0 = t_0^b/t_0^a$ ) as a groove which grows continuously by increasing the plastic strains to form finally from a localized neck. The imperfection factor can be presented as

$$f = \frac{t^b}{t^a} = f_0 \exp(\varepsilon_3^b - \varepsilon_3^a) \quad (15)$$

In Eq. (15)  $t$  and  $\varepsilon_3$  are the thickness and strain in thickness direction respectively which this strain can be defined in term of  $\varepsilon_1$  and  $\varepsilon_2$ .

$$\varepsilon_3 = -(\varepsilon_1 + \varepsilon_2) \quad (16)$$

Moreover, it is assumed that the homogeneous region exposes under proportional loading and increment of strains in groove direction are same in both homogeneous (a) and inhomogeneous (b) regions. During the deformation process, the angle of groove is a function of strains increment in the homogeneous region and can be derived in any step of loading according to [29].

$$\tan(\theta + d\theta) = \tan(\theta) \frac{1 + d\varepsilon_1^a}{1 + d\varepsilon_2^a} \quad (17)$$

Figure (1) shows the schematic of M-K model with normal stress. Applying the rotation matrix,  $R$ , the stress and strain tensor in regions (a) can be calculated in the groove coordinates.

$$R = \begin{bmatrix} \cos(\theta) & \sin(\theta) & 0 \\ -\sin(\theta) & \cos(\theta) & 0 \\ 0 & 0 & 1 \end{bmatrix} \quad (18)$$

$$[\sigma^a]_{ntz} = \begin{bmatrix} \sigma_{nn}^a & \sigma_{nt}^a & 0 \\ \sigma_{nt}^a & \sigma_{tt}^a & 0 \\ 0 & 0 & \sigma_{zz}^a \end{bmatrix} = R[\sigma^a]_{xyz}R^T \quad (19)$$

Post-print of "SM Mirfalah-Nasiri, A Basti, [R Hashemi](#) (2016) Forming limit curves analysis of aluminum alloy considering the through-thickness normal stress, anisotropic yield functions and strain rate, International Journal of Mechanical Sciences, Volume 117, Pages 93-101.

<https://doi.org/10.1016/j.ijmecsci.2016.08.011>

$$[d\varepsilon^a]_{ntz} = R[d\varepsilon^a]_{xyz}R^T \quad (20)$$

The un-known parameters including  $\sigma_{nn}^b, \sigma_{tt}^b, \sigma_{nt}^b$  and  $d\varepsilon^b$  can be derived from strain compatibility equation, energy equation, and two force equilibrium equations.

$$F_1 = \frac{d\varepsilon_{nn}^b \sigma_{nn}^b + d\varepsilon_{tt}^b \sigma_{tt}^b + d\varepsilon_{nt}^b \sigma_{nt}^b + d\varepsilon_3^b \sigma_3^b}{d\varepsilon^b \bar{\sigma}_Y^b} - 1 = 0$$

$$F_2 = \frac{d\varepsilon_{tt}^b}{d\varepsilon_{tt}^a} - 1 = 0$$

$$F_3 = f \frac{\sigma_{nn}^b}{\sigma_{nn}^a} - 1 = 0$$

$$F_4 = f \frac{\sigma_{nt}^b}{\sigma_{nt}^a} - 1 = 0$$
(21)

Introducing the function and un-known vectors as following

$$[F] = [F_1 \quad F_2 \quad F_3 \quad F_4]^T \quad (22)$$

$$[X] = [\sigma_{nn}^b \quad \sigma_{tt}^b \quad \sigma_{nt}^b \quad d\varepsilon^b] \quad (23)$$

The Newton-Raphson numerical method is employed to solve the system of Eq. (21) as following procedure.

$$[X]_{i+1} = [X]_i + [dX]_i \quad (24)$$

$$[dX]_i = -[J]_{ij}^{-1} [F]_j \quad (25)$$

In Eq. (25) the Jacobin matrix,  $[J]_{ij}$ , is defined as

$$[J]_{ij} = \left[ \frac{\partial F_i}{\partial X_j} \right] \quad (26)$$

In many research, investigation of normal stress effect on forming limit diagram is considered by introducing the non-dimensional parameters according to.

$$\gamma = \frac{\sigma_3}{\sigma_1} \quad (27)$$

$$S = \frac{|\sigma_3|}{Y} \quad (28)$$

Based on M-K model it is assumed that the localized necking in sheet metal occurs when the equivalent strain increment in groove region reaches ten time that in safe region ones [30] and limiting strains are saved. Applying this process, the limiting strains are derived by changing the ratio of stress in the FLD. The formability of sheet metals can be evaluated by using of FLD and FLSD in the strain state and stress state respectively. After computation of limiting strains and effective strains, the effective stresses are obtained by using hardening law. The limiting stresses can be derived by determination of ratio of stress

Post-print of “SM Mirfalah-Nasiri, A Basti, [R Hashemi](#) (2016) Forming limit curves analysis of aluminum alloy considering the through-thickness normal stress, anisotropic yield functions and strain rate, International Journal of Mechanical Sciences, Volume 117, Pages 93-101.

<https://doi.org/10.1016/j.ijmecsci.2016.08.011>

using yield function. Extended stress-based forming limit diagram (XFLSD) is the equivalent stress curve with respect to the hydrostatic stress which is defined as below.

$$\sigma_e = \bar{\sigma} \quad (29)$$

$$\sigma_{hyd} = \sigma_m = \frac{\sigma_1 + \sigma_2 + \sigma_3}{3} \quad (30)$$

#### 4- Constitutive model

The extended Ludwik constitutive model in terms of strain rate and temperature can be used to describe the thermo-elasto-viscoplastic behavior material as following

$$\bar{\sigma} = K(T) \bar{\epsilon}^{n_L(T)} \left( \frac{\dot{\bar{\epsilon}}}{\dot{\bar{\epsilon}}_0} \right)^{m_L(T)} \quad (31)$$

where  $\bar{\sigma}$ ,  $K$ ,  $\bar{\epsilon}$ ,  $n_L$ ,  $m_L$  and  $\dot{\bar{\epsilon}}$  are the stress, a material constant, the plastic strain, the strain-hardening coefficient, strain-rate sensitivity parameter and the strain rate respectively. In addition,  $\dot{\bar{\epsilon}}_0$  is a constant taken equal to  $1 \text{ s}^{-1}$ . Based on tensile testing, the parameters of extended Ludwik equation for AA3104 at strain rates from  $10^{-3}/\text{s}$  to  $10^{-5}/\text{s}$  and in the as-cast condition are presented in Table. 4. The strain rate has no effect in the M-K model by considering of this constitutive model in disappearance of time increment [32]. To overcome this problem the Johnson–Cook material model can be used. To describe the flow stress of the material, the Johnson–Cook material model incorporating strain rate and temperature functions can be employed.

$$\bar{\sigma} = (A + B\bar{\epsilon}^n) \left( 1 + C \ln \left( \frac{\dot{\bar{\epsilon}}}{\dot{\bar{\epsilon}}_0} \right) \right) \left( 1 - \left( \frac{T - T_r}{T_m - T_r} \right)^m \right) \quad (32)$$

where  $A$ ,  $B$ ,  $n$ ,  $C$  and  $m$  are the initial yield strength of the material at room temperature, work hardening coefficient, power of strain hardening, strain-rate sensitivity coefficient and material constant in J-C equation respectively. Moreover,  $T$  is the current temperature,  $T_m$  is the melting temperature of the material and  $T_r$  is the room temperature.

#### 5-Results and discussion

The anisotropic characteristics of the AA3104-H19 aluminum alloy which is used in this study are presented in Table. 5. The numerical results of anisotropic yield stress predicted using three yield criterion including K-B, Yld96 and Yld2011 are obtained for AA3104-H19 aluminum alloy sheet metal and then are compared with experimental results of normalized uniaxial yield stress. The comparison of experimental results of Ref [28] and the present work, for AA3104-H19 aluminum alloy sheet metal establishes the more accuracy of the Yld2011 yield criterion prediction than the K-B and Yld96 yield criterion ones as depicted in figure (2).

Post-print of “SM Mirfalah-Nasiri, A Basti, [R Hashemi](#) (2016) Forming limit curves analysis of aluminum alloy considering the through-thickness normal stress, anisotropic yield functions and strain rate, International Journal of Mechanical Sciences, Volume 117, Pages 93-101.

<https://doi.org/10.1016/j.ijmecsci.2016.08.011>

The comparison of the r-value predicted by K-B, Yld96 and Yld2011 yield criterion and the experimental data of Ref [28] for AA3104-H19 aluminum alloy sheet metal is shown in figure (3). As depicted in figure (3), the Yld2011 yield criterion gives satisfactory accurate correspondence to experimental data rather than r-value prediction. Moreover, the K-B and Yld96 yield criterions give lower r-value than the experimental data at 45 and 90 degree with respect to rolling direction.

Comparison between the accuracy of different yield functions to predict the plastic behavior of sheet metals can be obtained by introducing the comparative deviation or relative deviation for yield strength and r-value. The definition of relative root mean square deviation of the yield strength state can be presented as [7].

$$\Delta\sigma = \frac{\sqrt{\sum_{i=0}^n (\sigma_i(e) - \sigma_i(\alpha))^2 / n}}{(\sigma_0 + 2\sigma_{45} + \sigma_{90})/4} \quad (33)$$

In Eq. (33)  $\sigma_i(e)$ ,  $\sigma_i(\alpha)$  and  $n$  are the experimental uniaxial yield strengths, predicted uniaxial yield strengths and the number of experimental data points respectively. The description of relative root mean square deviation of the r-value can be defined as

$$\Delta r = \frac{\sqrt{\sum_{i=0}^n (r_i(e) - r_i(\alpha))^2 / n}}{(r_0 + 2r_{45} + r_{90})/4} \quad (34)$$

In Eq. (32),  $r_i(e)$ ,  $r_i(\alpha)$  are the experimental and the predicted r-value respectively. The relative deviation of yield strength  $\Delta\sigma$  and relative deviation r-value  $\Delta r$  are depicted in figure (4). As illustrated in figure (4), in general, the relative deviation values for the r-values are higher than those of the yield strengths. In addition, employing Yld2011 yield function, the values of the relative deviation ( $\Delta\sigma$  and  $\Delta r$ ) are lower than the values for the other two yield functions. According to these results, one can concluded that using Yld2011 yield function presents more satisfactory results than K-B and Yld96 yield functions to predict the anisotropic plastic behavior of AA3104-H19 aluminum sheet metals.

Employing a Hollomon type of power law relationship based on uniaxial tension test along rolling direction for AA3104-H19, the hardening characteristic of the material is obtained from experimental stress-strain response as following

$$\bar{\sigma} = K\bar{\epsilon}^n \quad (35)$$

In Eq. (35)  $K = 390.4$  MPa and the strain hardening parameter  $n = 0.07$  [27]. Wu et al. [27] calculated the initial inhomogeneity coefficient by comparison between predicted FLDs and measured results and trial and error procedure for aluminum alloy AA3104-H19 as  $f_0 = 0.992$ . Soare [33] was proposed the analytical equation to calculate the initial inhomogeneity coefficient as following

Post-print of "SM Mirfalah-Nasiri, A Basti, [R Hashemi](#) (2016) Forming limit curves analysis of aluminum alloy considering the through-thickness normal stress, anisotropic yield functions and strain rate, International Journal of Mechanical Sciences, Volume 117, Pages 93-101.  
<https://doi.org/10.1016/j.ijmecsci.2016.08.011>

$$f_0 = \left( \frac{\varepsilon_x^T}{n} \right)^n \exp(n - \varepsilon_x^T) \quad (36)$$

Considering the target strain as  $\varepsilon_x^T = 0.042$  and the a power hardening law with  $n = 0.07$  for aluminum alloy AA3104-H19, the initial inhomogeneity coefficient can be calculated as  $f_0 = 0.9923$ . The comparison between the results of references [27] and [33] establishes the accuracy of predicted initial inhomogeneity coefficient. For this reason in this study the initial inhomogeneity coefficient was considered as  $f_0 = 0.992$ .

Prediction of forming limit diagram based on M-K model and different yield functions for AA3104-H19 under in plane stress is presented in figure (5). The remarkable difference between the theoretical prediction curve based on K-B, Yld96 and Yld2011 yield function can be observed in the tension-tension strain states described in the right hand side of the FLC. Moreover, the significant reduction ones can be found in the tension- compression strain states described in the left hand side of the FLD. Forming limit diagram prediction based on K-B yield criterion just verifies the experimental results of in plane strain state only and based on Yld96 yield criterion validates the experimental results in the vicinity of biaxial stress state described in the right hand side of the FLD. Moreover, as illustrated in figure (5), the Yld2011 yield criterion introduces the satisfactory accurate results in comparison to experimental data of Ref [27]. For this reason, the investigation of through-thickness normal compressive stress effect on formability of aluminum sheet metal is carried out by using of Yld2011 yield function. Figure (6) shows the sensitivity of the yield surface in the principle stress plane to through- thickness normal compressive stress. As illustrate in this figure, applying the normal compressive stress would cause the initial yield surface shifts along the equi-biaxial compression direction and principle in plane stress in tension-tension region reduced which results in the sheet metals formability increase.

The effect of different through-thickness normal compressive stress on the formability of AA3104-H19 aluminum alloy based on the modify M-K model and Yld2011 yield function is investigated and illustrated in figure (7). The FLDs were predicted for a normal compressive stress ranging from plane stress condition ( $\gamma = 0$  to  $\gamma = -0.45$ ). Applying the normal compressive stress on the sheet metals, the in plane biaxial tension stresses decreases as reported the previous researches. For this reason, the formability of AA3104-H19 increases by increasing of through-thickness normal compressive stress as shown in figure (7). Table. 7 presents the considerable increasing in  $FLD_0$  with increasing the absolute of normal compressive stress according to the following relation.

$$\zeta = \frac{FLD_{0 \text{ with existence of normal stress}} - FLD_{0 \text{ plane stress}}}{FLD_{0 \text{ plane stress}}} \times 100 \quad (37)$$

Post-print of "SM Mirfalah-Nasiri, A Basti, [R Hashemi](#) (2016) Forming limit curves analysis of aluminum alloy considering the through-thickness normal stress, anisotropic yield functions and strain rate, International Journal of Mechanical Sciences, Volume 117, Pages 93-101.

<https://doi.org/10.1016/j.ijmecsci.2016.08.011>

The effect of through-thickness normal compressive stress on formability of AA3104-H19 aluminum alloy in stress based forming limit diagram is depicted in figure (8). Despite of an upward shift in strain based forming limit diagram by increasing the absolute compressive normal stress, the downward shift is observed in stress based forming limit diagram. In fact, the normal compressive stress causes a reduction in the yield surface and principle stress in tension-tension region. For this reason, FLSD reduces and the formability of sheet metals increase. The effective stress in term of the normal stress depends on loading type (strain path) which different strain paths (i.e. between uniaxial tension and equibiaxial tension) can have different effects on the effective stress. The normal stress influence on the extended stress-based forming limit curve (XFLSD) is presented in figure (9).

Based on Ludwik equation and the presented parameters of table. 4, the true stress–strain responses of AA3104 at strain rate  $10^{-4} \text{ s}^{-1}$  for different temperature are presented in figure (10). The results show that the negative temperature sensitivity on the stress-strain curve. The comparison between the results of reference [31] and the present study shows the accuracy of the theory in predicting the stress-strain response. Using the stress-strain response corresponding to the Ludwik model at  $300 \text{ }^\circ\text{C}$  for different strain rate and presented numerical procedure in reference [23], the five J-C parameters are obtained of AA3104, As depicted in figure (11). The results show that, by increasing the strain rate from  $10^{-5}$  to  $10^{-3} \text{ s}^{-1}$ , the true stress-true strain response of AA3104 at  $300 \text{ }^\circ\text{C}$  increases.

Comparison between experimental FLD of Al 6061-T6 of reference [22] and present analytical FLD are presented in figure (12) to verify the present procedure by using of J-C model corresponding to Al 6061-T6. Satisfactory accuracy can be observed the predicted analytical and experimental FLD at different strain rate at quasi-static, intermediate and high strain rate conditions. After this verification, the new results of FLD of AA3104 by using the corresponding J-C coefficient, presented in figure (11), and by considering strain rate effect are analytically investigated and depicted in figure (13). As shown in figure (13), the negative strain rate sensitivity can be concluded at quasi-static conditions and at  $300 \text{ }^\circ\text{C}$ .

The influence of temperature in range of  $50 \text{ }^\circ\text{C}$  to  $500 \text{ }^\circ\text{C}$  on the FLD of AA3104 by using of Ludwik model is illustrated in figure (14). It is found that the material shows the positive temperature sensitivity on FLD of AA3104 sheets. The stress based forming limit diagram for AA3104 at different temperatures and at strain rate  $10^{-4} \text{ s}^{-1}$  is depicted in figure (15). The results show that, increasing the temperature the FLSD decreases and the formability increases.

## **6-Conclusion**

In this article the effect of through-thickness normal stress investigation according to Yld2011 yield criterion and modified Marciniak–Kuczynski (M–K) model to predict the stress-based forming limit curve, strain based forming limit curve and extended forming limit stress diagram was studied. The

Post-print of "SM Mirfalah-Nasiri, A Basti, [R Hashemi](#) (2016) Forming limit curves analysis of aluminum alloy considering the through-thickness normal stress, anisotropic yield functions and strain rate, International Journal of Mechanical Sciences, Volume 117, Pages 93-101.

<https://doi.org/10.1016/j.ijmecsci.2016.08.011>

Newton–Raphson numerical method is employed to solve the set of nonlinear equations to calculate limited strains. The prediction of anisotropic plastic behavior of aluminum alloy AA3104-H19 by Yld2011 yield criterion was compared with available experimental data and prediction results of K-B and Yld96 yield functions. The effect of strain rate is investigated on true stress-true strain curve and FLD of AA3104 by using of J-C constitutive law at quasi-static condition. Moreover, based on Ludwik model, the influence of temperature on the true stress-true strain response, FLD and FLSD of AA3104 is studied.

The key findings of the present work are summarized as follows

- 1- The anisotropic plastic behavior of AA3104-H19 aluminum alloy predicted by Yld2011 yield criterion introduces a good agreement with experimental data.
- 2- The Yld2011 yield function gives more satisfactory accurate results than the K-B and Yld96 yield functions to predict the FLC with in plane stress condition especially in tension- compression strain states described in the left hand side of the FLC.
- 3- Considering the through-thickness normal compressive stress effect, the limiting strain in plane strain state increases 35 percent by applying the stress ratio of  $\gamma = -0.45$ .
- 4- Increasing of strain rate increases the stress-strain response and decreases the FLD of AA3104 sheets metal.
- 5- The FLSD exhibit the negative temperature sensitivity of AA3104 alloy.

## References

- [1] Keeler, S. P. and Backofen, W. A.: Plastic instability and fracture in sheets stretched over rigid punches, Transactions of the American Society for Metals, 56, 25-48, 1963.
- [2] Goodwin G. M.: Application of strain analysis to sheet metal forming problems in the press shop, Society of Automotive Engineers, 680093, 380-387, 1968.
- [3] Marciniak, Z. and Kuczynski, K.: Limit strains in the processes of stretch forming sheet metal, International Journal of Mechanical Sciences, 9, 609-620, 1967.
- [4] Marciniak, Z., Kuczynski, K. and Pokora, T.: Influence of the plastic properties of a material on the forming limit diagram for sheet metal in tension, International Journal Mechanical Sciences, 15, 789-805, 1973.
- [5] Butuc, M. C., Banabic, D., Barata da Rocha, A. and Gracio, J. J.: The performance of Yld96 and BBC2000 yield functions in forming limit prediction, Journal of Materials Processing Technology, 125, 281-286, 2002.
- [6] Ganjiani, M. and Assempour, A.: An improved analytical approach for determination of forming limit diagrams considering the effects of yield functions, Journal of Materials Processing Technology, 182, 598-607, 2007.

- Post-print of "SM Mirfalah-Nasiri, A Basti, [R Hashemi](#) (2016) Forming limit curves analysis of aluminum alloy considering the through-thickness normal stress, anisotropic yield functions and strain rate, International Journal of Mechanical Sciences, Volume 117, Pages 93-101.  
<https://doi.org/10.1016/j.ijmecsci.2016.08.011>
- [7] Ahmadi, S., Eivani, A. R. and Akbarzadeh, A.: An experimental and theoretical study on the prediction of forming limit diagrams using new BBC yield criteria and M-K analysis, Computational Materials Science, 44, 1272-1280, 2009.
- [8] Dasappa, P., Inal, K. and Mishra, R.: The effects of anisotropic yield functions and their material parameters on prediction of forming limit diagram, International Journal of Solids and Structures, 49, 3528-3550, 2012.
- [9] Li, X., Song, N., Guo, G. and Sun, Zh.: Prediction of forming limit curve (FLC) for Al-Li alloy 2198-T3 sheet using different yield functions, Chinese Journal of Aeronautics, 26, 1317-1323, 2013.
- [10] Panich, S., Barlat, F., Uthaisangskuk, V., Suranuntchai, S. and Jirathearant, S.: Experimental and theoretical formability analysis using strain and stress based forming limit diagram for advanced high strength steels, Materials and Design, 51, 756-766, 2013.
- [11] Ozturk, F., Toros, S. and Kilic, S.: Effects of anisotropic yield functions on prediction of forming limit diagrams of DP600 advanced high strength steel, Procedia Engineering, 81, 760-765. 2014.
- [12] Bridgman, P. W.: Studies in large plastic flow and fracture, McGraw-Hill, New York, 1952.
- [13] Fuchs, P. J.: Hydrostatic pressure: its role in metal forming, Mechanical Engineering, 34-40, 1966.
- [14] Assempour, A., Khakpour Nejadkhaki, H. and Hashemi, R.: Forming limit diagrams with the existence of through-thickness normal stress, Computational Materials Science, 48, 504-508, 2010.
- [15] Hashemi, R. and Abrinia, K.: Analysis of the extended stress-based forming limit curve considering the effects of strain path and through-thickness normal stress, Materials and Design, 54, 670-677, 2014.
- [16] Nurcheshmeh, M. and Green, D. E.: The effect of normal stress on the formability of sheet metals under non-proportional loading, International Journal of Mechanical Sciences, 82, 131-139, 2014.
- [17] Zhang, F., Chen, J., Chen, J. and Zhu, X.: Forming limit model evaluation for anisotropic sheet metals under through-thickness normal stress, International Journal of Mechanical Sciences, 89, 40-46, 2014.
- [18] Zhang, F., Chen, J. and Chen, J.: Effect of through-thickness normal stress on forming limits under Yld2003 yield criterion and M-K model, International Journal of Mechanical Sciences, 89, 92-100, 2014.
- [19] Yang, X., Lang, L., Liu, K. and Guo, C.: Modified MK model combined with ductile fracture criterion and its application in warm hydroforming, Transactions Nonferrous Metals Society of China, 25, 3389-3398, 2015.
- [20] Kim, S.B., Huh, H., Bok, H.H. and Moon, M.B.: Forming limit diagram of auto-body steel sheets for high-speed sheet metal forming, Journal of Materials Processing Technology, 211, 851-862, 2011.
- [21] Gerdoee, M. and Dariani, B. M.: Strain-rate-dependent forming limit diagrams for sheet metals, Journal of Engineering Manufacture, 222 (B), 1651-1659, 2008.

Post-print of "SM Mirfalah-Nasiri, A Basti, [R Hashemi](#) (2016) Forming limit curves analysis of aluminum alloy considering the through-thickness normal stress, anisotropic yield functions and strain rate, International Journal of Mechanical Sciences, Volume 117, Pages 93-101.

<https://doi.org/10.1016/j.ijmecsci.2016.08.011>

- [22] Dariani, B. M., Liaghat, G. H. and Gerdoee, M.: Experimental investigation of sheet metal formability under various strain rates, Journal of Engineering Manufacture, 223 (B),703-712,2009.
- [23] Khan, A. S. and Biag, M.: Anisotropic responses, constitutive modeling and the effects of strain-rate and temperature on the formability of an aluminum alloy, International Journal of Plasticity, 27, 522–538, 2011.
- [24] Chu, X., Leotoing, L., Guines, D. and Ragneau, R.: Temperature and strain rate influence on AA5086 Forming Limit Curves: Experimental results and discussion on the validity of the M-K model, International Journal of Mechanical Sciences, 78, 27–34, 2014.
- [25] Zhang, C., Chu, X., Guines, D., Leotoing, L., Ding, J. and Zhao, G.: Dedicated linear-Voce model and its application in investigating temperature and strain rate effects on sheet formability of aluminum alloys, Materials & Design, 67, 522-530, 2015.
- [26] Banabic, D.: Sheet metal forming processes constitutive modeling and numerical simulation, Springer, Germany, 2010.
- [27] Wu, P. D., Jain, M., Savoie, J., MacEwen, S. R., Tugcu, P. and Neale, K. W.: Evaluation of anisotropic yield functions for aluminum sheets, International Journal of Plasticity, 19, 121-138, 2003.
- [28] Aretz, H. and Barlat, F.: New convex yield functions for orthotropic metal plasticity, International Journal of Non-Linear Mechanics, 51, 97-111, 2013.
- [29] Sowerby, R and Duncan, D. L.: Failure in sheet metal in biaxial tension, International Journal of Mechanical Science, 217-229, 1971.
- [30] Barata da Rocha, A., Barlat, F. and Jalinier, J. M.: Prediction of the forming limit diagrams of Anisotropic sheets in linear and non-linear loading, Materials Science and engineering, 151-164,1985.
- [31] Van Haafte, W.M., Magnin, B., Kool, W.H. and Katgerman, L.: Constitutive Behavior of As-Cast AA1050, AA3104, and AA5182, Metallurgical and Materials Transactions A, 33, 1971-1980, 2002.
- [32] Zhang, C., Leotoing, L., Guines, D. and Ragneau, E.: Theoretical and numerical study of strain rate influence on AA5083 formability, Journal of Materials Processing Technology, 2009, 3849–3858, 2009.
- [33] Soare, S. C.: Theoretical considerations upon the MK model for limit strains prediction: the plane strain case, strain-rate effects, yield surface influence, and material heterogeneity, European Journal of Mechanics / A Solids, 29, 938-950, 2010.

Post-print of "SM Mirfalah-Nasiri, A Basti, [R Hashemi](#) (2016) Forming limit curves analysis of aluminum alloy considering the through-thickness normal stress, anisotropic yield functions and strain rate, International Journal of Mechanical Sciences, Volume 117, Pages 93-101.

<https://doi.org/10.1016/j.ijmecsci.2016.08.011>

#### List of captions:

##### Figure caption

Fig. 1. A detailed view of the M–K model considering the normal stress effect.

Fig. 2. Comparison of predicted directional yield strength and experimental data for AA3104-H19 alloy.

Fig. 3. Comparison of predicted directional r-values and experimental data for AA3104-H19 alloy.

Fig. 4. Yield strength and r-value comparative deviations for different yield functions.

Fig. 5. Comparison of experimental and theoretical FLDs obtained by using various yield function under plane-stress condition for AA3104-H19 sheet metal.

Fig. 6. Effects of normal stress on initial yield surfaces in the principle stress plane for AA3104-H19.

Fig. 7. Effects of the normal stress on prediction FLDs for AA3104-H19 aluminum alloy.

Fig. 8. Effects of the through-thickness normal stress on FLSDs considering Yld2011 yield criterion for AA3104-H19 sheet.

Fig. 9. Effects of the normal stress on XFLSDs considering Yld2011 for AA3104-H19 alloy.

Fig. 10. Comparing stress-strain response of AA3104 in the present work at strain rate  $10^{-4}$  /s to that reported by Haafte et al. [31].

Fig. 11. True stress–true strain response of AA3104 at 300°C along with correlation from Johnson-Cook model.

Fig. 12. Comparing strain rate response of Al6061-T6 in the present work to that reported by Dariani et al. [22].

Fig. 13. The effect of strain rate on FLD of AA3104 at 300°C by using Johnson-Cook model.

Fig. 14. The effect of temperature on FLD of AA3104 in quasi-static condition by using Ludwik model.

Fig. 15. The effect of temperature on FLSD of AA3104 in quasi-static condition by using Ludwik model.

##### Table caption

Table (1) Yld96 yield function parameters for the aluminum alloy AA3104-H19 ( $a=8$ ) [27].

Table (2) K-B yield criterion parameters for AA3104-H19 ( $a=30$ ,  $c=0.164$ ) [27].

Table (3) Yld2011-18p yield function parameters for aluminum AA3104-H19 ( $a=12$ ) [28].

Table (4) Parameters of Ludwik model for AA3104 at strain rates from  $10^{-3}$  /s to  $10^{-5}$  /s (quasi-static condition)[31].

Table (5) Anisotropy characteristics of the AA3104-H19 aluminum alloy [28].

Table (6) Percentage of FLD<sub>0</sub> increase " $\zeta$ " for different values of " $\gamma$ " function.

**Highlights:**

- 1- Directional normalized uniaxial yield stresses, directional r-value and forming limit curve for AA3104-H19 alloy under plane stress condition are investigated by employing three anisotropic yield criteria, including Karafillis-Boyce, Yld96 and Yld2011.
- 2- The Marciniak–Kuczynski model is modified by considering the through-thickness normal stress.
- 3- Based on the Yld2011 yield criterion, the effect of through-thickness normal stress is studied on the FLD, FLSD and XFLSD.
- 4- The anisotropic plastic behavior and FLC of AA3104-H19 predicted by Yld2011 yield criterion is in good agreement with experimental data and is more accurate than those of K-B and Yld96 yield functions.
- 5- The investigation of strain rate and temperature effects on the FLD of AA3104 shows the negative strain rate sensitivity and positive temperature sensitivity.

Fig. 1.

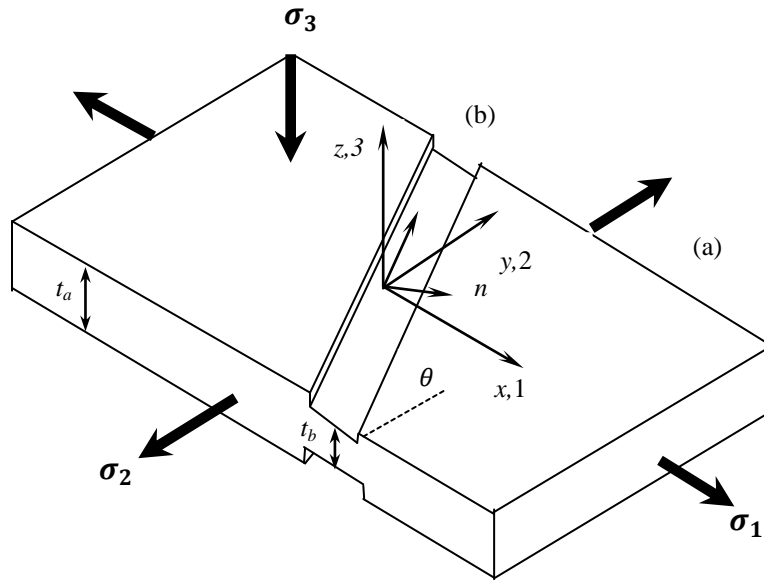


Fig. 2.

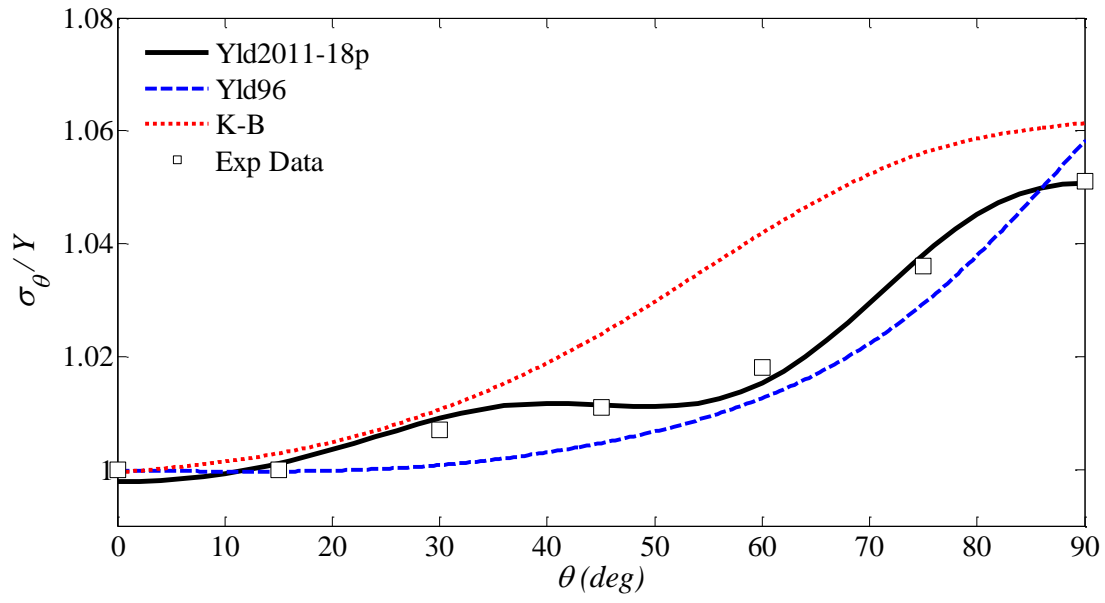


Fig. 3.

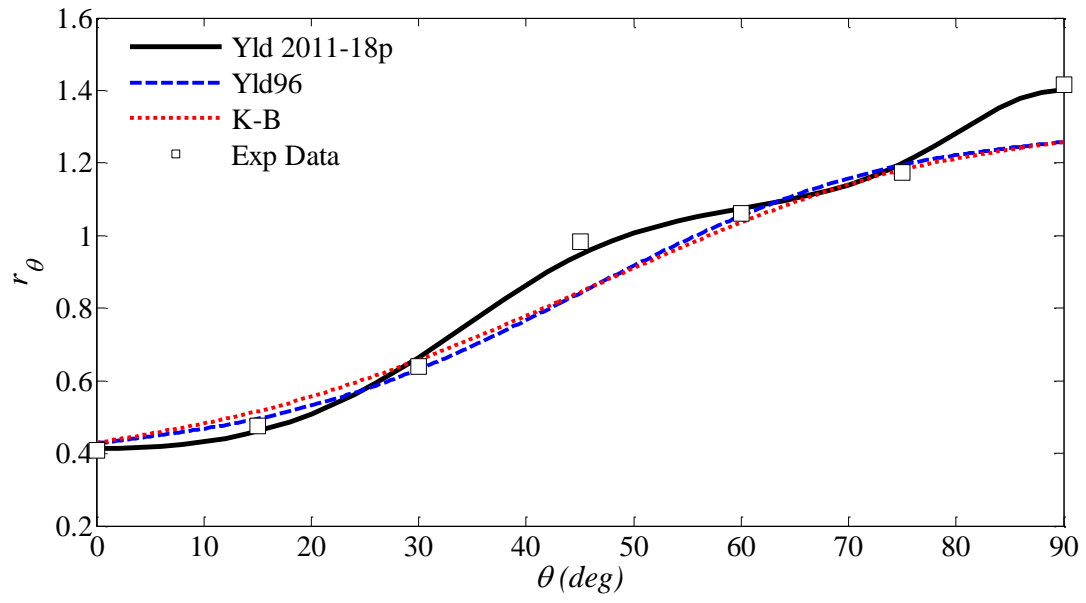


Fig. 4.

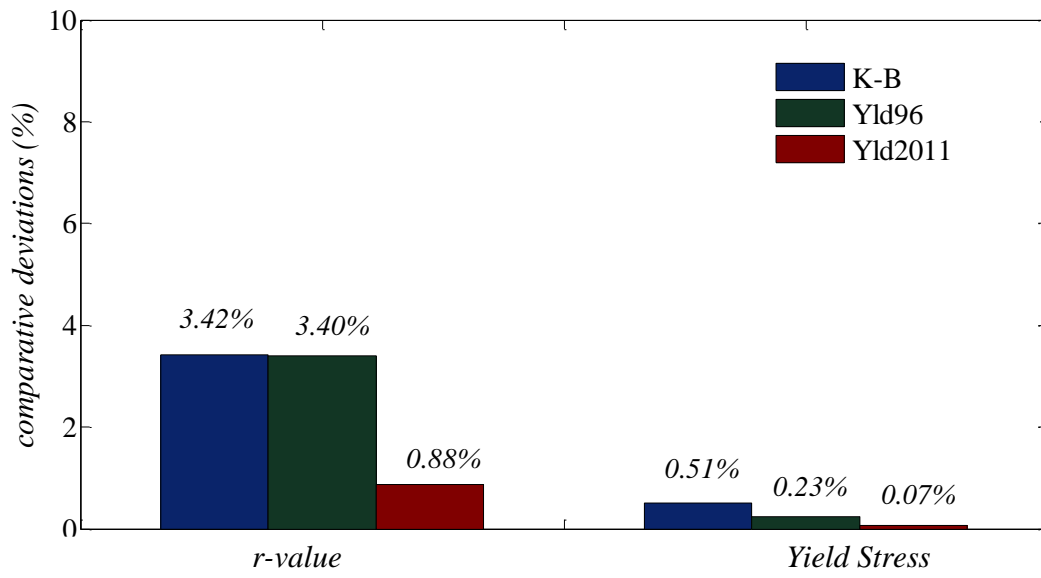


Fig. 5.

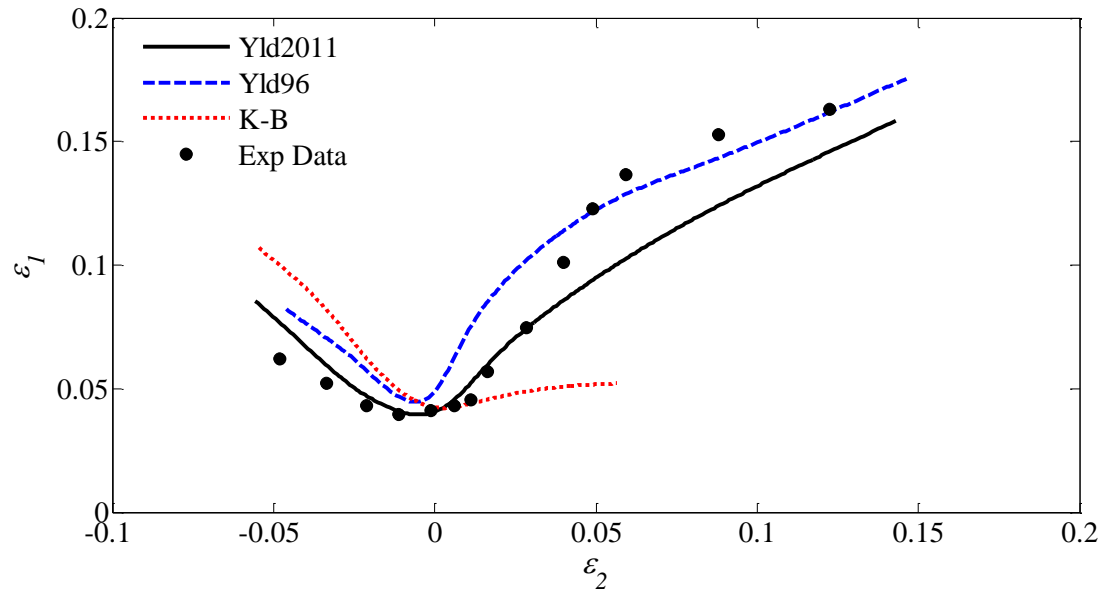


Fig. 6.

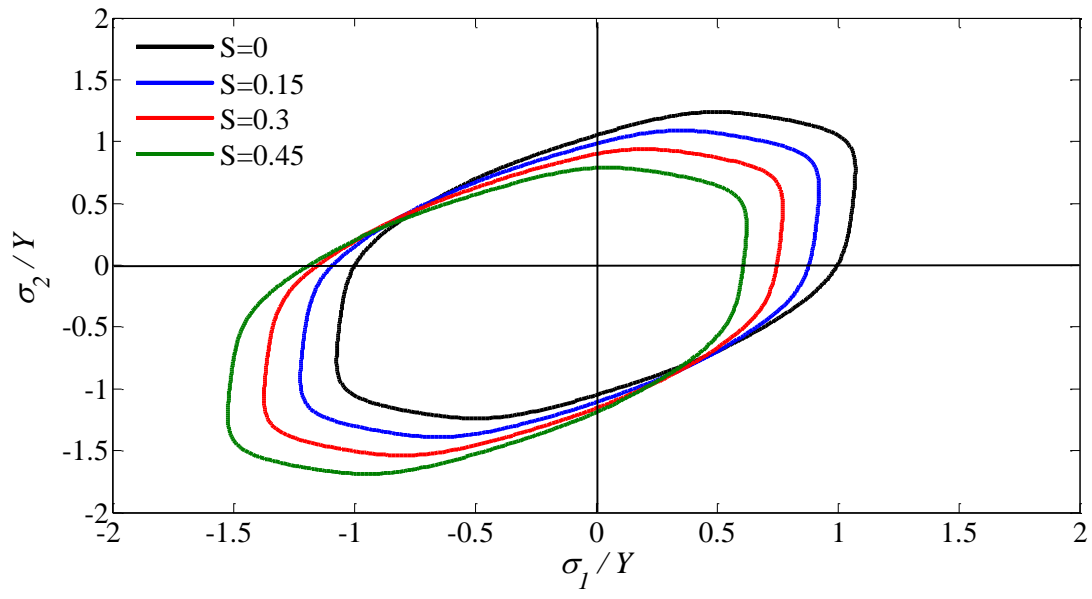


Fig. 7.

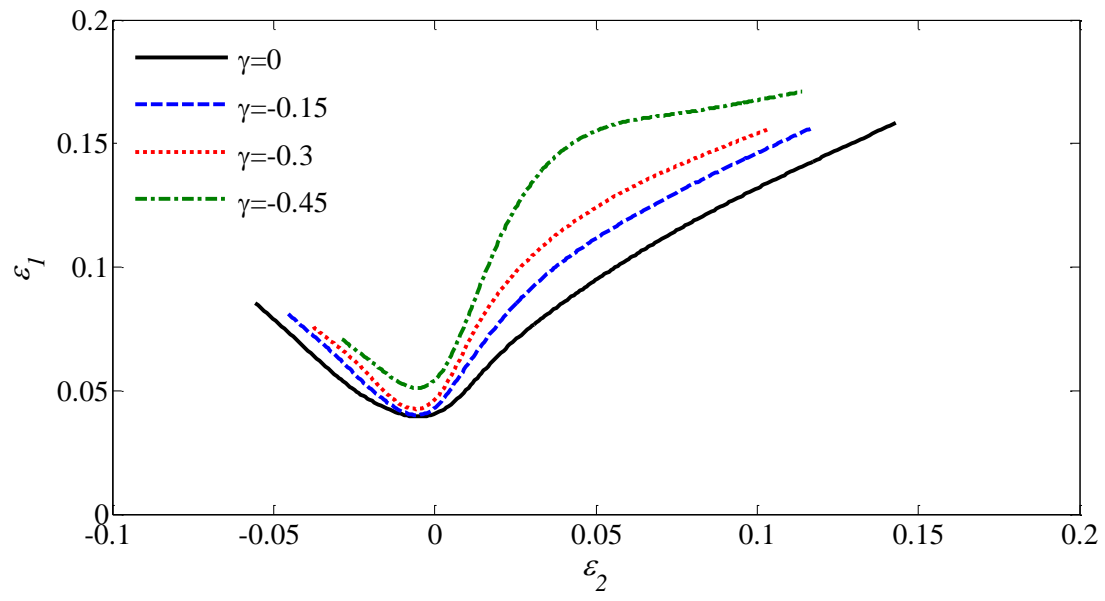


Fig. 8.

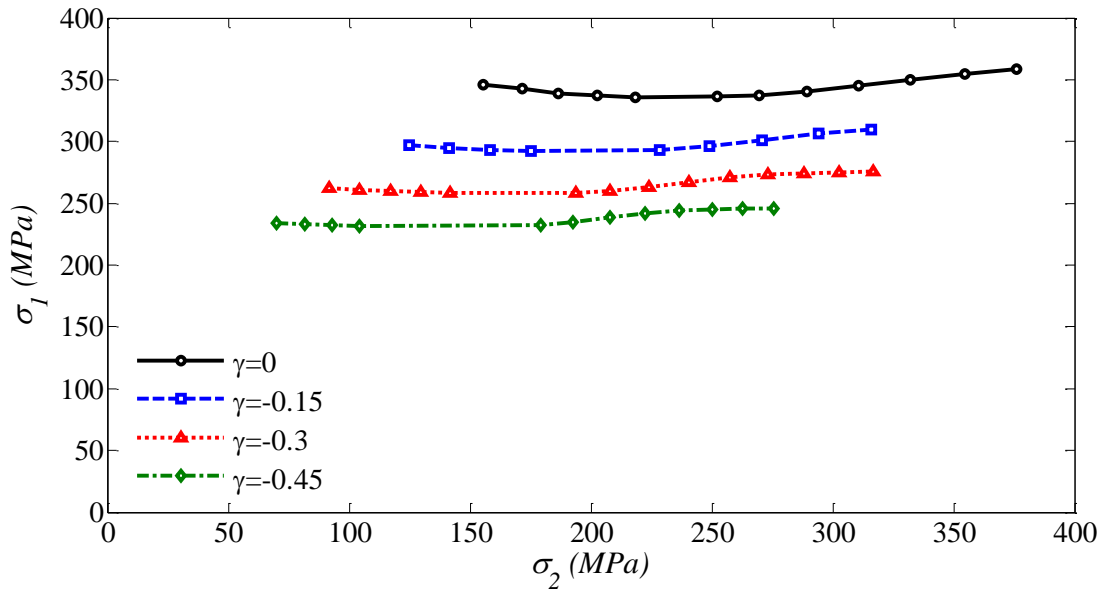


Fig. 9.

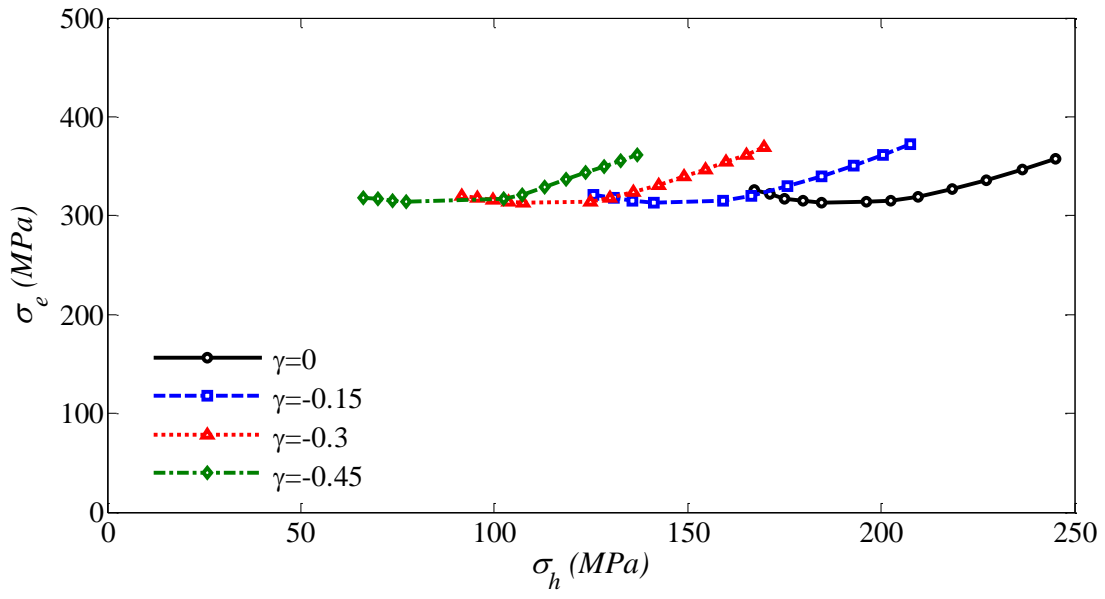


Fig. 10.

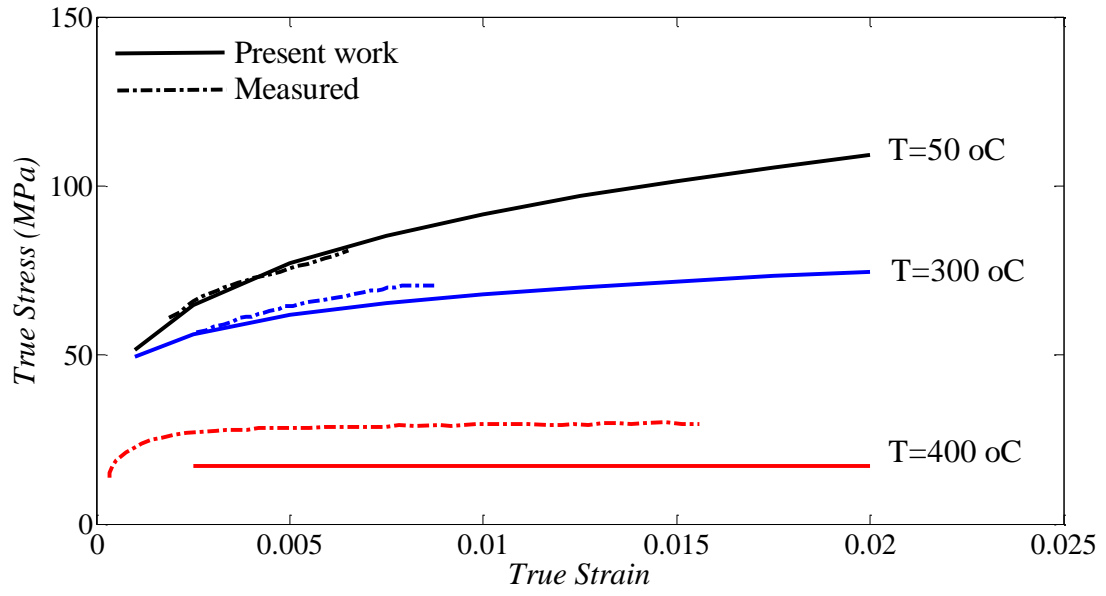


Fig. 11.

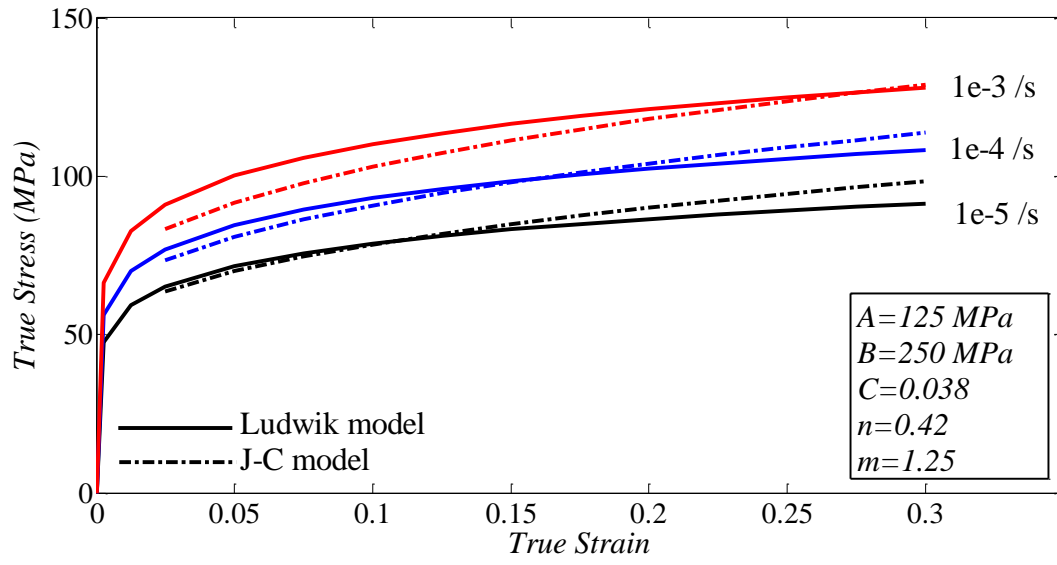


Fig. 12.

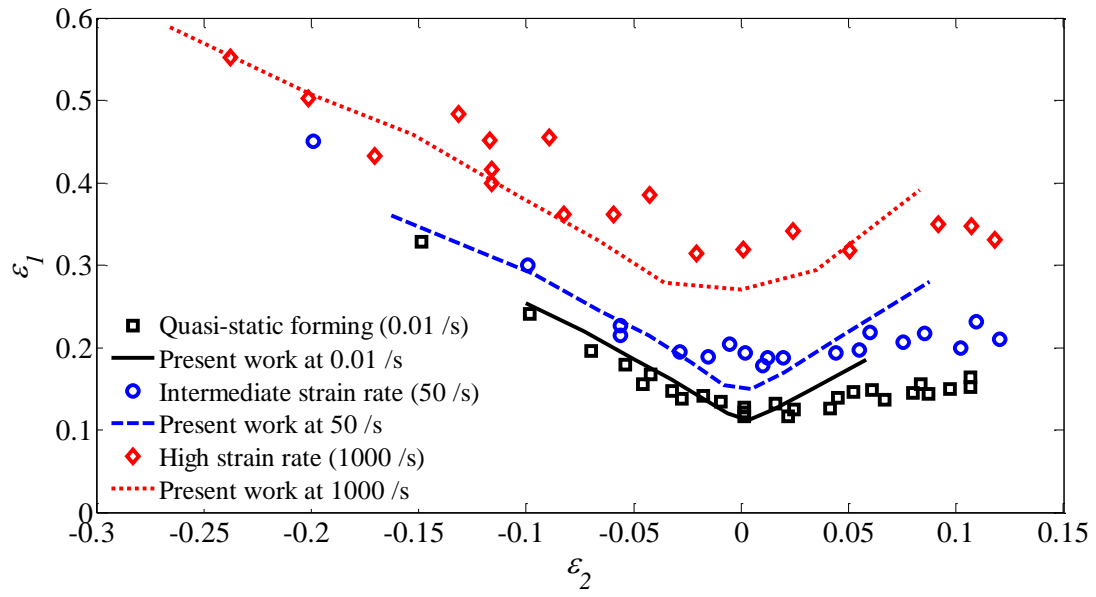


Fig. 13.

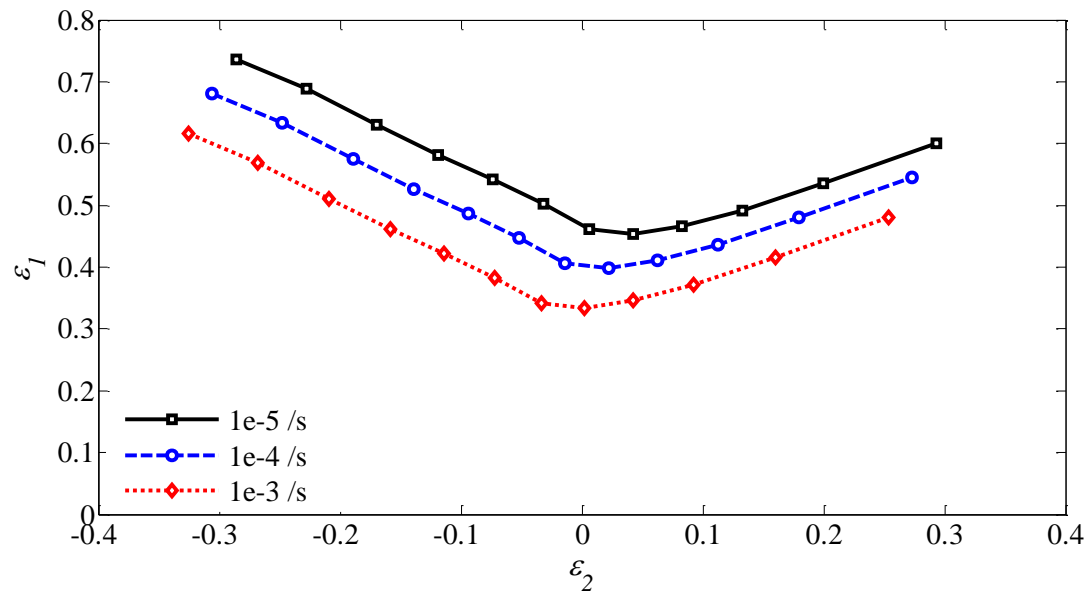


Fig. 14.

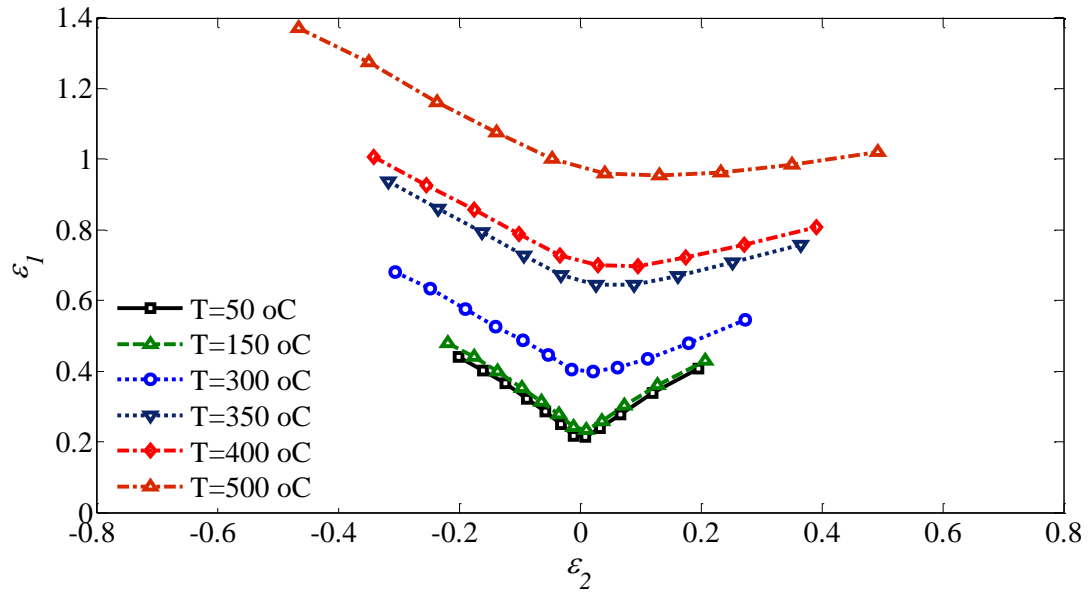


Fig. 15.

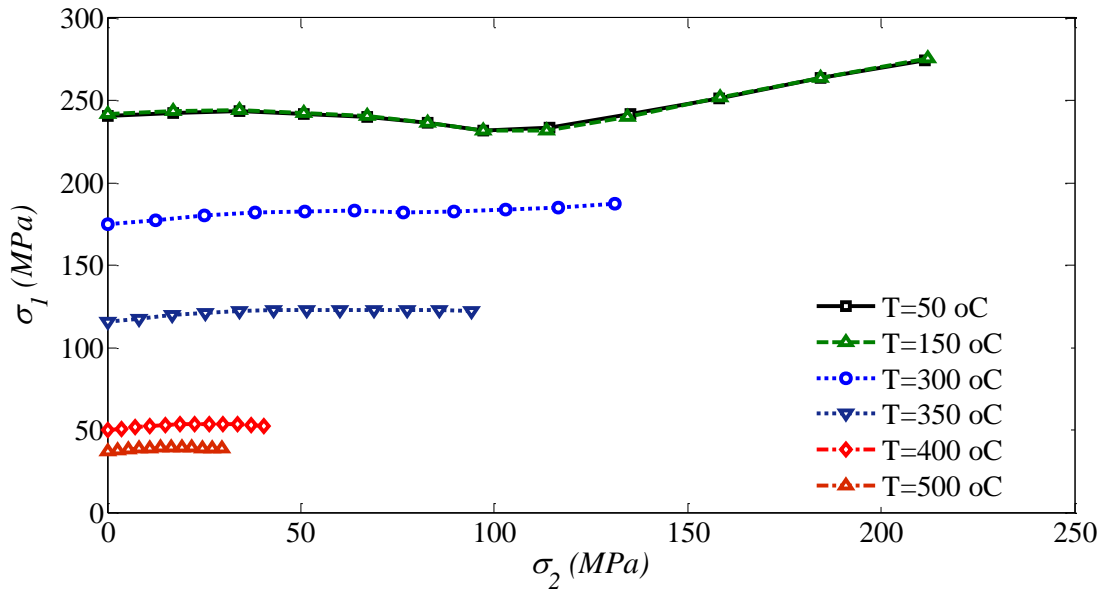


Table 1.

$c_1$	$c_2$	$c_3$	$c_4$	$c_5 = c_6$
1.047	0.9329	0.8985	0.8941	1
$\alpha_{x0} = \alpha_{x1}$	$\alpha_{y0} = \alpha_{y1}$		$\alpha_{z0}$	$\alpha_{z1}$
0.4706	1.892		1	1.056

Table 2.

$c_1$	$c_2$	$c_3$	$c_4$	$c_5 = c_6$
0.9265	1.0451	0.9488	0.9733	1

Table 3.

$C'_{12}$	$C'_{13}$	$C'_{21}$	$C'_{23}$	$C'_{31}$	$C'_{32}$	$C'_{44}$	$C'_{55}$	$C'_{66}$
1.28025	0.853723	0.758983	1.5	1.63180	1.45339	1	1	0.880608
$C''_{12}$	$C''_{13}$	$C''_{21}$	$C''_{23}$	$C''_{31}$	$C''_{32}$	$C''_{44}$	$C''_{55}$	$C''_{66}$
0.795767	0.715288	1.18774	0.315233	-0.0608724	0.693975	1	1	1.19887

Table 4.

<b><i>T</i></b> (°C)	<b>50</b>	<b>100</b>	<b>150</b>	<b>200</b>	<b>250</b>	<b>300</b>	<b>350</b>	<b>400</b>	<b>450</b>	<b>500</b>
<b><i>K</i></b> (MPα)	290	273	290	268	260	250	240	117	102	107
<b><i>n<sub>L</sub></i></b>	0.250	0.265	0.272	0.247	0.237	0.137	0.039	0	0	0
<b><i>m<sub>L</sub></i></b>	0	0	0	0	0	0.073	0.179	0.209	0.249	0.270

Table 5.

Uniaxial tensile test data:							
$\theta(^{\circ})$	0	15	30	45	60	75	90
$r_{\theta}$	0.408	0.475	0.639	0.984	1.060	1.173	1.416
$\frac{Y_{\theta}}{Y}$	1.000	1.000	1.007	1.011	1.018	1.0361	1.051

Table 6.

<b>Material</b>	<b><math>\gamma</math></b>	<b><math>\zeta</math> (%)</b>
	-0.15	4.7
<b>AA3104-H19</b>	-0.3	15.2
	-0.45	35.1